# Bending Fatigue Behavior of Differently Heat Treated and Shot Peened AlCu5Mg2

T. Hirsch, O. Vöhringer, E. Macherauch

*Institut für Werkstoffkunde I*
*Universität Karlsruhe*
*D-7500 Karlsruhe, FRG*

ABSTRACT

The effect of different shot peening and heat treatments on the cyclic bending fatigue behavior of a precipitation hardenable aluminum alloy of the type AlCu5Mg2 was investigated. Depending on the material states different increases in fatigue life and bending fatigue limit were obtained. The amounts of increase can be considered to be mainly a result of the surface work hardening and surface residual stresses. The surface roughness is of minor importance. Shot peening residual stresses become less stable with increasing loading stress. They were reduced especially during the first load cycle. The relaxation rate depends on initial surface residual stresses, on the stress amplitude and on the surface yield strength. The latter can be determined by combined quasistatic tension and compression tests as well as by X-ray measurements.

KEYWORDS

Aluminum alloy, shot peening, bending fatigue behavior, residual stresses and relaxation of residual stresses.

## INTRODUCTION

It is known that shot peening influences the fatigue behavior of metals by changing the material states of surface layers (see e.g. Butz, 1961; Snowman, 1981, Person, 1981). Systematic investigations of the effect of shot peening-caused changes on the residual stress and work hardening state in surface layers have not been carried out so far. Besides a few indications (Potter, 1977) it is unknown to which extent cyclic loading reduces shot peening residual stresses in age-hardenable aluminum alloys. Furthermore, practically no research has been done on the influence of shot peening on the fatigue behavior of purposely varied heat treatment conditions.

The influence of different shot peening pressures and shot types on the bending fatigue behavior of the aluminum alloy AlCu5Mg2 in the as-received condition and two additional heat treatments is demonstrated by this paper. The material's state will always be described by measurements of residual stresses, half width and hardness as well as surface roughness. Furthermore,

experimental results about relaxation of residual stresses under different amplitudes are described. Finally, the results of additional research about relaxation of residual stresses in shot peened specimens under quasistatic tensile and compressive loading are shown.

## EXPERIMENTAL DETAILS

The investigations were obtained from the aluminum alloy AlCu5Mg2 (chemical composition 4.54 % Cu; 1.43 % Mg; 0.1 % Si; 0.2 % Fe; 0.85 % Mn; 0.035 % Zn and 0.014 % Ti -all units in wt-%-). Shape and size of the specimens are shown in Fig. 1. The specimens were taken out of rolled sheet material of 20 mm thickness and, with the exception of that in the as-received condition, were solution annealed at 495 °C for two hours and quenched in water of 15 °C. Aging treatments followed for 30 days at 20 °C (under-aging) and 12 h at 190 °C (peak-aging). Immediately after the treatment the specimens were shot peened and then cyclically loaded. Electropolished specimens were used for comparison measuring with not shot peened material states.

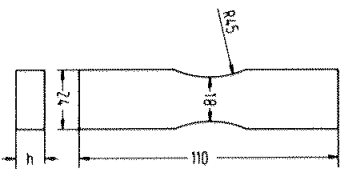


Fig. 1: Shape and size of the fatigue specimens (h = 2 mm)

Some of the specimens in the as-received condition were shot peened in an air blast machine. The shot peening treatments are summarized in Table 1. A cast iron shot with a hardness of 46-50 HRC was used. 98 % coverage was chosen for all experiments.

| shot type | steel balls | | | glass beads |
|---|---|---|---|---|
| shot size [mm] | 0,43 (S 170) | | | 0,125 - 0,250 |
| peening pressure [bar] | 0,2 | 0,45 | 1,2 | 0,8 |
| coverage [ % ] | 98 | 98 | 98 | 98 |
| Almen "A" intensity [mm] | 10 | 20 | 30 | 8 |
| density of shot per area [g/mm²] | 0,3 | 0,25 | 0,15 | 0,008 |

Table 1: Shot peening conditions

The residual stresses of the samples were determined by X-ray measurement with a $\psi$-diffractometer (Wolfstieg, 1976) and by the so-called $\sin^2\psi$ method (Macherauch, 1961) with copper $K\alpha$-radiation. Therefore, the residual lattice strains of {511/333} -planes were measured from the shifts of the appertaining interference line profiles in specified directions $\psi$ against the surface normal. To improve the grain statistics all samples were subjected to translation (+ 10 mm) and rotation (2-3 degrees around the specimens' longitudinal axis) during the measurement. Residual stress distributions were determined by measuring electrochemically removed material layers with

different distances from the surface. The measured data were corrected for the disturbance of the existing residual stress state (Moore, 1958). Measurements of the half width of the X-ray interference line profiles and hardness tests gave information about the work hardening of the near surface layers. A characteristic residual stress distribution of a specimen shot peened with S 170 and p = 1.2 bar is shown in Fig. 2a. Typical distributions of half width and hardness are represented in Fig. 2b. The cyclic loading was applied in one load stage in mechanically driven bending fatigue machines (model Schenck) with a sinusoidal load-time-function. Six samples were tested for each of five suitably chosen stress levels. The limit of the number of cycles for non-fractured specimens having passed the fatigue test was set to be $10^7$. In the low cycle region as well as in the high cycle region the experimental data were interpreted with the arc sin $\sqrt{P}$ transformation method (Dengel, 1975) with P being the probability of fracture. As an example, Fig. 2c shows the result of the Woehler diagram (SN-curve) determined for the shot peening conditions S 170 and p = 1.2 bar. The diagram contains SN-curves for probabilities of fracture of 95 %, 50 % and 5 %.

## RESULTS

First, the influence of the shot peening pressure and with this different Almen-intensities for constant shot type (S 170) on the material states of the near surface layers was investigated. In Fig. 3a corresponding residual stress distributions are shown. The depth of the maxima of the compressive residual stresses as well as their penetration depth increase with increasing peening pressure. Half width and hardness increase at the surface and in near surface layers with increasing peening pressure, as demonstrated in Fig. 3b. The bending fatigue limit also increases with increasing pressure as can be seen in Fig. 3c. In the low cycle region only for small stress amplitudes an increase in the fatigue life with increasing pressure could be observed. Characteristic data are summarized in Table 2: the surface compressive residual stresses $\sigma_{RS,S}$ the half width $HWB_S$, the hardness HV $0.1_S$, the roughness $R_t$ and $R_a$ as well as the bending fatigue limit for a probability of fracture of 50 %.

| condition | $\sigma_{RS,S}$ [N/mm²] | $HWB_S$ [min] | HV $0.1_S$ | $R_t$ [µm] | $R_a$ [µm] | fatigue limit [N/mm²] |
|---|---|---|---|---|---|---|
| electropolished | - 50 ± 18 | 220 ± 9 | 159 ± 18 | 2,6 | 0,3 | 115 |
| S 170, p=0,2bar 10 A [mm] | -332 ± 5 | 309 ± 8 | 255 ± 23 | 16 | 2,1 | 138 |
| S 170, p=0,45bar 20 A [mm] | -340 ± 6 | 334 ± 13 | 261 ± 31 | 27 | 3,8 | 150 |
| S 170, p=1,2bar 30 A [mm] | -292 ± 6 | 343 ± 12 | 290 ± 28 | 51 | 6,8 | 153 |
| glass beads d=0,125-0,25mm p=0,8bar 8 A [mm] | -317 ± 9 | 315 ± 6 | 252 ± 36 | 20 | 2,6 | 139 |

Table 2:

Characteristic surface values and fatigue limits of shot peened as well as elektropolished specimens in the as-received condition

In Fig. 4 experimental results are shown received for a comparable Almen-intensity after shot peening treatments with steel balls and glass beads respectively. As can be seen, almost identical distributions of residual

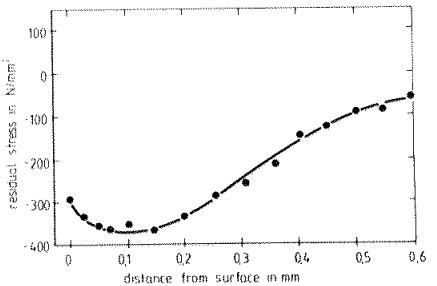


Fig. 2a

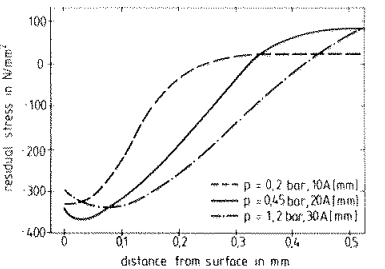


Fig. 3a

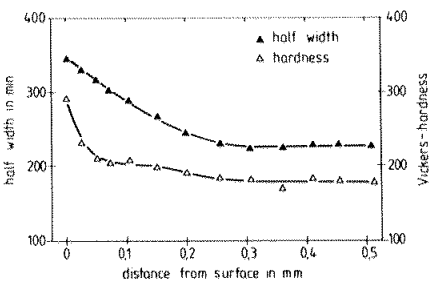


Fig. 2b

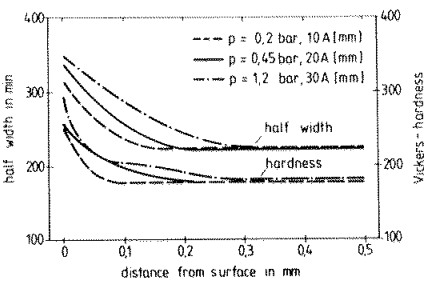


Fig. 3b

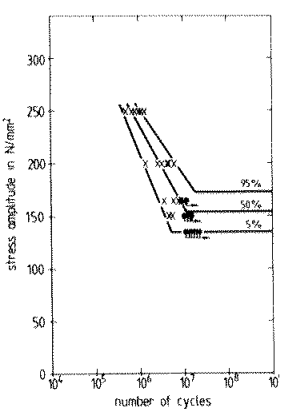


Fig. 2c

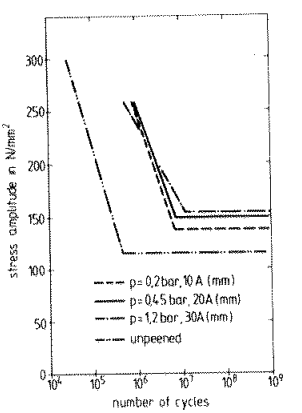


Fig. 3c

Fig. 2:
Characteristic data distributions measured

a) shot peening residual stresses
b) half width and hardness
c) appertaining SN-curves

Fig. 3:
Distributions of

a) residual stresses
b) half width and hardness
c) appertaining SN-Curves of different peening pressures (S 170 and 98 % coverage = const)

stresses are resulting (Fig. 4a) as well as similar half width and hardness distributions (Fig. 4b) with a good correspondence of the surface values. The fatigue limits also correspond well in both cases. Table 2 summarizes characteristical numerical values of the discussed results.

Similar results to the ones already reported for the heat treated and shot peened conditions are given in Fig. 5 and Table 3. For a shot peening treatment with S 170, p = 1.2 bar, 98 % coverage and 30 A [mm] in the under-aged condition a residual stress distribution similar to the as received condition was observed (Fig. 5a). Compared to these samples the peak-aged condition shows values for residual stresses that are smaller by almost a factor of 2. At the surface and in near surface layers there are clearly smaller values for half-width and hardness after peak-aging than after under-aging. This is illustrated in Fig. 5b. The largest values for half-width and hardness were found for the shot peened state of the as-received condition. Compared to the polished samples (not shot peened), the fatigue limits of all shot peened samples were increased after any of the described treatments. This can be read from Fig. 5c and the data given in Table 3. The values for the surface roughness increase considerably after the shot peening treatment. This is documented in columns 6 and 7 in Table 3. The shot peening-caused increase of the fatigue life is considerably smaller for the peak-aged condition than for any of the other two conditions. The under-aged condition shows the largest bending fatigue limit.

| condition | $R_{p0,2}$ [N/mm²] | $R_m$ [N/mm²] | $\sigma_{RS,s}$ [N/mm²] | $HWB_s$ [min] | HV 0,1$_s$ | $R_t$ [µm] | $R_a$ [µm] | fatigue limit [N/mm²] |
|---|---|---|---|---|---|---|---|---|
| as-received + polished | 394 | 496 | -50 ± 18 | 220 ± 9 | 159 ± 18 | 2,6 | 0,3 | 115 |
| 20 °C/ 30 d + polished | 391 | 471 | -12 ± 6 | 180 | 147 ± 4 | 2,6 | 0,3 | 132 |
| 190 °C/12 h + polished | 407 | 480 | - 1 ± 5 | 190 | 149 ± 8 | 3,4 | 0,4 | 121 |
| as-received + shot peened | -- | -- | -292 ± 6 | 343 ± 12 | 290 ± 28 | 51 | 6,8 | 153 |
| 20 °C/30 d + shot peened | -- | -- | -308 ± 13 | 331 ± 6 | 208 ± 9 | 43 | 6,3 | 183 |
| 190 °C/12 h + shot peened | -- | -- | -167 ± 11 | 262 ± 3 | 163 ± 7 | 48 | 6,6 | 165 |

Table 3: Characteristic surface values and fatigue limits of shot peened (S 170, p = 1.2 bar, 98 % coverage and 30 A [mm]) as well as electropolished specimens in different conditions

For stress amplitudes higher than $\sigma_a$ = 150 N/mm² changes of residual stresses with an increasing number of cycles occur for all material- and peening conditions investigated. Characteristic examples are shown in Fig. 6a-c separately for the initially tension loaded and the initially compression loaded side of the specimen. In general, a high stress amplitude means a large decrease of residual stresses. The highest changes of residual stresses always occured during the first load cycle. The compression load cycle caused the largest relaxation effect. Only for the peak- aged condition for N > 1 changes of the residual stresses can be found.

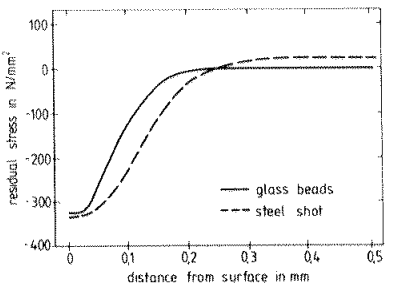


Fig. 4a

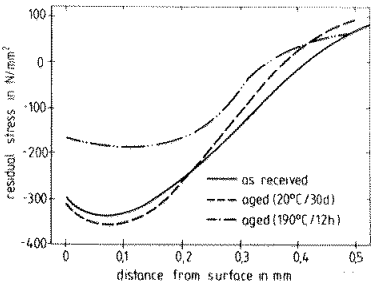


Fig. 5a

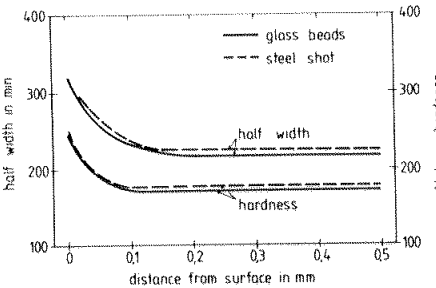


Fig. 4b

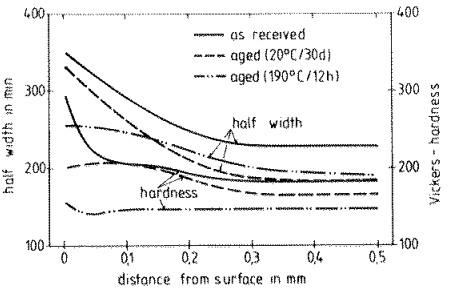


Fig. 5b

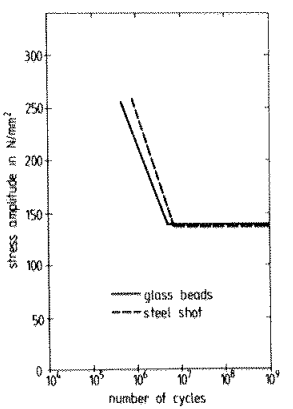


Fig. 4c

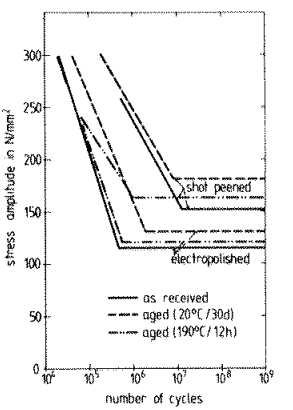


Fig. 5c

Fig. 4: Distribution of

a) residual stresses
b) half width and hardness
c) appertaining SN-curves after steel shot and glass bead peening of similar Almen-intensity 10 A [mm] and 8 A [mm] respectively

Fig. 5: Distributions of

a) residual stresses
b) half width and hardness
c) appertaining SN-curves of of shot peened specimens (S 170, p = 1.2 bar, 98 % coverage and 30 A [mm]) in three different conditions

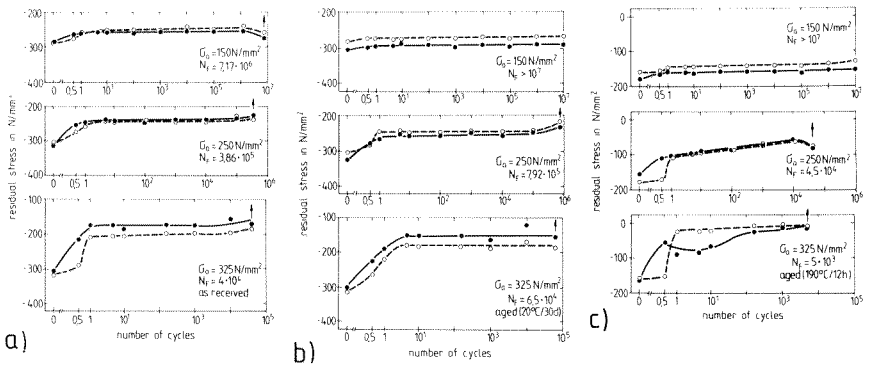


Fig. 6: Shot peening residual stresses versus number of cycles for a) as-received, b) under-aged and c) peak-aged condition (shot peened with S 170, p = 1.2 bar, 98 % coverage and 30 A [mm]) (o--first tensile side,●— first compressive side)

For a better understanding of the residual stress relaxation (shortened as RRS) during the first load cycle of the bending fatigue loading additional experiments about the RRS during homogeneous tension and compression loading were conducted. In Fig. 7a-c the residual stresses versus total deformation after tension and compression loading were shown. Specimens of different sample conditions were shot peened with S 170, p = 1.2 bar and 98 % coverage. Furthermore, in Fig. 8a-c residual stresses after tension or compression with characteristic yield stresses are shown as a function of the maximum loading stress. The residual stresses of shot peened speci-

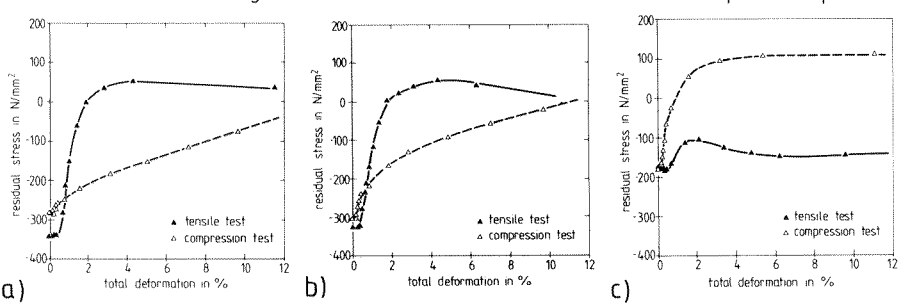


Fig. 7: Residual stresses versus total deformation under quasistatic loading for a)as-received, b) under-aged and c) peak-aged condition (shot peened with S 170, p = 1.2 bar, 98 % coverage and 30 A [mm])

mens in the as-received condition decrease with tension loading after a total extension of $\varepsilon_t \geq 0.5$ % (maximum loading stress $\sigma$ above 320 N/mm$^2$). For $\varepsilon_t$ larger than 2 % the residual stresses disappear completely. For $\varepsilon_t \approx 2$ % tension residual stresses develop. The compression test results in a decrease of residual stresses above $\varepsilon_t = -0.25$ % (maximum loading

stress $\sigma \sim -175$ N/mm$^2$). The relaxation rate is much smaller than for the tension test. A similar behavior is found for the under-aged state. Above $\varepsilon_t = 0.3$ % ($\sigma \approx 220$ N/mm$^2$) for the tension test and $\varepsilon_t = -0.1$ % ($\sigma \approx -75$ N/mm$^2$) for the compression test RRS starts (Fig. 7b, 8b). The peak-aged material state, however, shows a completely different behavior of its RRS. After passing a total extension of $\varepsilon_t = 0.5$ % ($\sigma \approx 275$ N/mm$^2$) only a minor loss of residual stresses occurs during the tension test. However, during the compression test residual stresses decrease much faster for a total deformation of $\varepsilon_t = -0.1$ % than in the as-received or under-aged condition.

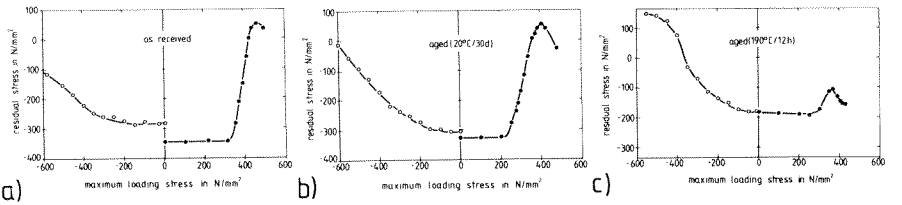


Fig. 8: Residual stresses versus maximum loading stress under quasistatic loading for a) as-received, b) under-aged and c) peak-aged condition (shot peened with S 170, p = 1.2 bar, 98 % coverage and 30 A [mm])

## DISCUSSION

It is widely accepted that shot peening caused improvements of the fatigue behavior of metallic materials is a result of the coexistence of surface residual stresses, surface work hardening and surface roughness effects. For materials with low strength the influence of work hardening predominates for materials with medium strength the influence of work hardening and compressive residual stresses is about equal, and for hard materials the influence of compressive residual stresses and surface roughness on fatigue life and fatigue limit is dominant (Schreiber, 1976, Starker, 1981).

In the as-received condition of the alloy investigated the fatigue behavior is determined apparently by surface work hardening and shot peening residual stresses as the results in Fig. 3 and Table 2 support. For small stress amplitudes the bending fatigue limit as well as the fatigue life increase with increasing half width of X-ray interference line profiles and increasing surface hardness, regardless of the much increased surface roughness and decreasing values for the surface residual stresses. Another possible reason for the extended fatigue life is the increase in depth of compressive residual stresses with increasing air pressure (Fig. 3). For stable residual stress conditions the crack growth is slowed down over a longer distance in the crack propagation phase. In addition, a reduction of the crack growth rate can be expected with growing amount of compressive residual stresses.

For cyclic loading of technical aluminum alloys in differently heat treated states crack initiation at brittle inclusions predominates (Grosskreutz, 1967/68; Hunter, 1955; Haworth, 1977; Heinzelmann, 1982). The different heat treatment induced types of precipitations and therefore different possibilities of movement and interaction of dislocations result in less cycles to crack initiation and larger crack growth rates for the peak aged condi-

tion and, therefore, the fatigue behavior is not as good as for the under-aged state (Calabrese, 1974; Laird, 1977; Park, 1971; Schulz, 1978). The results displayed in Fig. 5c for electropolished specimens in under-aged and peak-aged conditions agree well with that. The as-received condition which was obtained by hot rolling immediately followed by aging at room temperature has the lowest bending fatigue limit. It is possible that the high dislocation density in this state (note comparatively large half width values in Table 3), affected by the sheet production, and distinct dislocation arrangements are responsible for this behavior. After shot peening longer fatigue lives in the low cycle fatigue region and higher bending fatigue limits could be observed as compared to the polished specimens. The order of the bending fatigue limits for the heat treatments remains the same. In other words, the fatigue strengths increase from the as-received condition to the peak-aged and finally to the under-aged condition, although the different material states have different states of residual stresses and work hardening. The observed increases in fatigue strength have to be interpreted in different ways. In the as-received condition as well as for the under-aged state as compared to the peak-aged condition basically the rather large surface work hardening and high shot peening residual stresses cause the increase in fatigue limit. On the other hand, the large surface roughness has to be considered reductive on fatigue strength because it supports crack initiation for a high micro notch sensitivity. For a comparable degree of roughness this micro notch sensitivity has a stronger negative influence on the higher strength material states which are the as-received and the peak-aged condition. With this in mind, the obtained largest increase in the bending fatigue limit of $\sim 50\ N/mm^2$ for the under-aged specimens becomes more reasonable (Table 3).

In the low cycle region the fatigue life for as-received and under-aged material conditions can be increased by shot peening by about an order of magnitude (see Fig. 5c). However, the observed $N_F$ growth for the peak-aged condition is surprisingly small. The rather small shot peening work hardening and the by a factor of 2 smaller amounts of residual stresses are responsible for that. In addition, the residual stresses have an even lower effect on cyclic loading, because they were partially or completely reduced before failure, depending on the loading stress (Fig. 6c).

Besides the amount and the distribution of the shot peening residual stresses the stability of these residual stresses is of special interest for the fatigue behavior of the shot peened AlCu5Mg2 alloy. As Fig. 6 shows, the shot peening residual stresses are reduced if the stress amplitude is high enough. The highest decay of the amount of compressive residual stresses happens during the first half load cycle. The behavior observed here is comparable to the quasistatic tension and compression loading of shot peened specimens. In these cases RRS occurs after reaching a critical value for the maximum loading stress with corresponds to a relatively small total deformation (Fig. 7,8). For the following a shot peened slim specimen is described as compound with a work hardened surface segment with compressive residual stresses, characterized by the surface yield strength $R_{es}{}^R$ and the surface residual stress $\sigma_{RS}{}^R$, and a not work hardened core segment with tension residual stresses, characterized by the core yield strength $R_{es}{}^K$ and the core residual stress $\sigma_{RS}{}^K$. For such a model the tension yield strength $\bar{R}_{es,t}$ under tensile loading can be calculated using a linear superposition of the axial loading- and the axial residual stresses with

$$\bar{R}_{es,t} = R_{es}{}^K - \sigma_{RS}{}^K \qquad (1)\ \text{(Vöhringer, 1983)}$$

A similar relation for the compression yield strength under compression loading is

$$\overline{R}_{es,c} = R_{es}^{R} - |\sigma_{RS}^{R}| \qquad (2) \quad \text{(Vöhringer, 1983)}$$

The surface- and core residual stresses $\sigma_{RS}^{R}$ and $\sigma_{RS}^{K}$ are the residual stresses existing after shot peening. However, only $\sigma_{RS}^{R}$ can be determined experimentally. The average yield strengths $R_{es,t}$ and $\overline{R}_{es,c}$ can be obtained experimentally from Fig. 8 as maximum loading stresses for beginning RRS. Therefore, an estimation of the surface yield strength was possible with Eq. (2): $R_{es}^{R}$ = 515 N/mm² for the as-received, $R_{es}^{R}$ = 466 N/mm² for the under-aged condition and $R_{es}^{R}$ = 285 N/mm² for the peak-aged condition. Since $R_{es}^{K}$ corresponds to the matrix yield strength (see Table 3 for $R_{p0.2}$-values) $R_{es}^{R}$ is greater than $R_{es}^{K}$ for the shot peened material in the as-received and the under-aged state. Therefore, the shot peened surface is work hardened as compared to the core. For the peak-aged condition, however, the condition $R_{es}^{R} < R_{es}^{K}$ is valid. Here it is a work softened surface state as compared to the core.

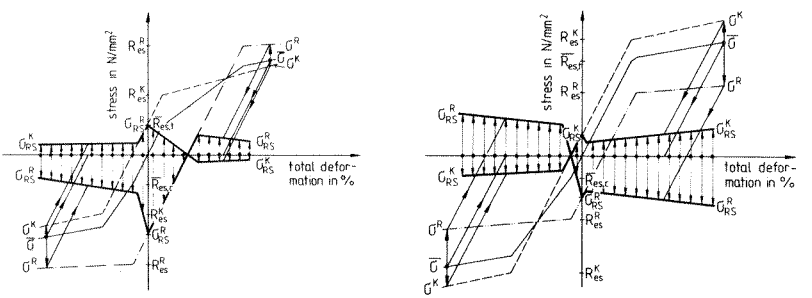


Fig. 9: Schematic load-total strain diagram for the relaxation of residual stresses under quasistatic tension and compressive loading
a) as-received condition
b) peak-aged condition

In Fig. 9a the load-total strain diagram is drawn schematically for a compound of core segment and strain hardened surface segment ($R_{es}^{K} < R_{es}^{R}$) under the assumption of linear static strain hardening of the compound. In Fig. 9b the equivalent diagram for a compound of core and work hardened surface layer ($R_{es}^{K} > R_{es}^{R}$) is drawn. After overelastic tension and compression loading, respectively, and following load relief reduced and reorientated residual stresses are present. The amount of the reduction of residual stresses is determined by the deformation inhomogeneity between surface and core segment. The shown relaxation behavior describes the different experimental observations for the as-received as well as for the under-aged and peak-aged condition quantitatively correct.

Because of these models after bending fatigue loading of shot peened AlCu5Mg2 specimens with a stress amplitude of $\sigma_a$ = 150 N/mm² only a small

RRS can be expected during the first load cycle for all conditions (see Fig. 6 and Fig. 8). For $\sigma_a$ = 325 N/mm² the average yield strengths were passed at the compression as well as tension loaded side of the fatigue specimens already during the first half load cycle (see Fig. 6 and Fig. 8). Therefore, RRS occurred for all conditions to different degrees on both sides of the specimen. For the number of cycles N greater than 1 essentially no further RRS could be observed, with the exception of the peak-aged condition. For the peak-aged condition further RRS occurred which could be a result of rearrangements of dislocations and/or formation of cracks.

The most important parameters determining the RRS during cyclic loading are therefore stress amplitude $\sigma_a$, initial surface residual stresses $\sigma_{RS}{}^R$ and surface yield strength $Res^R$. Fig. 10 summarizes these influences on the RRS after N = $N_F$. On the left side of Fig. 10 the initial residual stresses ($\sigma_a$ = 0) and the residual stresses after failure during loading with different stress amplitudes $\sigma_a$ are shown for the investigated conditions of AlCu5Mg2 (upper 3 curves). Some data for other shot peened materials are included in Fig. 10 for comparison. With increasing $\sigma_a$ and $\sigma_{RS}{}^R$ the RRS becomes more pronounced. If the surface yield strength $R_{eS}{}^R$ is known, the ratio of final to original residual surface stress $\sigma_{RS}(F)/\sigma_{RS}(0)$ can be determined as a function of the ratio of applied stress amplitude to surface yield strength $\sigma_a/R_{eS}R$. The left side of Fig. 10 shows that in bending fatigue this function is practically the same for all materials, regardless materials state and treatment.

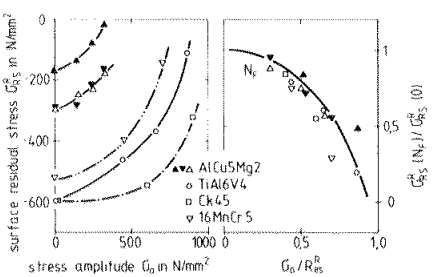


Fig. 10:

Surface residual stresses and $\sigma_{RS}{}^R(N_F)/\sigma_{RS}{}^R(0)$ respectively versus stress amplitude and $\sigma_a/R_{es}{}^R$ respectively

(△: as received, ▼: under-aged, ▲: peak-aged; □: Starker, 1981; ▽: Schreiber, 1976)

REFERENCES


Butz, G.A. and Lyst, J.O.: Mat. Res. and Standards 12, 1961, p. 951-956

Calabrese, C. and Laird, C.: Mat. Sci. and Engineering 13, 1974, p. 141-174 and 159-174

Dengel, D.: Z. f. Werkstofftechnik 6, 1975, p. 253-261

Grosskreutz, J.C.: Mat. Sci. and Engineering 2, 1967/68, p. 249-261

Haworth, W.L.; Hieber, A.F. and Mueller, R.K.: Met. Trans., Vol. 8A, 1977, p. 1597-1604

Heinzelmann, P.: Studienarbeit, Universität Karlsruhe, 1982

Hunter, M.S. and Fricke, W.G.: ASTM Proceedings, Vol. 55, 1955, p. 942-953

Laird, C.: ASTM STP 637, 1977, p. 3-35

Macherauch, E. and Müller, P.: Z. f. angewandte Physik 13, 1961, p. 305-312

Moore, M.G. and Evans, W.P.: Trans SAE, 66, 1958, p. 341-345

Park, B.K.; Luetjering, G. and Weissmann, S.: Z. Metallkunde 62, 1971, p. 721-726

Person, N.L.: Metal Progress 7, 1981, p. 33-35
Potter, J.M. and Millard, R.A.: Adv. in X-Ray Analysis, Vol. 20, 1977, p. 309-319
Schreiber, R.: Dr.-Ing.-Dissertation, Universität Karlsruhe, 1976
Schulz, H. and Knoblauch, H.: Aluminium, 54, 1978, p. 561-566
Starker, P.: Dr.-Ing. Dissertation, Universität Karlsruhe, 1981
Snowman, A. and Schmidt, R.G.: 1st Int. Conf. on Shot Peening, Pergamon Press, 198 , p. 313-319
Vöhringer, O.: in "Eigenspannungen, Entstehung-Berechnung-Messung-Bewertung," Deutsche Gesellschaft für Metallkunde, Oberursel, 1983
Wolfstieg, U.: Härterei-Technische Mitteilungen 31, 1976, p. 19-22